Electronic Supplementary Material (ESI) for Soft Matter.

Capillary forces drive buckling, plastic deformation, and break-up of 3D printed beams

Christopher S. O'Bryan[1,2], Alexandria Brady-Mine[2], Crystal J. Tessmann[2], Amanda M. Spotz[2], Thomas E. Angelini[2,3,4,5,*]

[1] Department of Chemical and Biomolecular Engineering, University of Pennsylvania, Philadelphia, PA, USA
[2] Department of Mechanical and Aerospace Engineering, Herbert Wertheim College of Engineering, University of Florida, Gainesville, FL, USA
[3] Department of Material Engineering, Herbert Wertheim College of Engineering, University of Florida, Gainesville, FL, USA
[4] J. Crayton Pruitt Family Department of Biomedical Engineering, Herbert Wertheim College of Engineering, University of Florida, Gainesville, FL, USA
[5] Institute of Cell & Tissue Science and Engineering, Herbert Wertheim College of Engineering, University of Florida, Gainesville, FL, USA

[*] Corresponding Author: t.e.angelini@ufl.edu

1. Methods

1.1. Aqueous Microgels

Aqueous microgel samples are prepared by swelling Ashland 980 carbomer in deionized water (Millipore) at the given polymer concentration. The dry polymer is dispersed by speed-mixing the sample for 15 min at 3500 RPM (FlakTek DAC 150.1). Swelling of the microgel particles is achieved by adjusting the pH of the solution to ~7 through the addition of 1N NaOH (Fisher Scientific). The samples are left to equilibrate overnight. Prior to use, the samples are speed-mixed for 30 s at 3000 RPM to remove air bubbles trapped within the packed microgels.

1.2. Organic Microgels and Micelles

Organic microgels swollen in neat mineral oil are prepared through the self-assembly of polystyrene-*block*-polyethylene/propylene (SEP) diblock copolymers (KRATON G1702; MW 172.6 kg/mol, polydispersity 1.03; density: 0.91 g/mL) and polystyrene-*block*-polyethylene/butylene-*block*-polystyrene (SEBS) triblock copolymers (KRATON 1650; MW 98.1 kg/mol, polydispersity 1.03; density: 0.91 g/mL) in NF/FCC light mineral oil (Fisher Scientific; density: 0.838 g/mL). Micro-organogels are prepared at 2.3 wt% SEP diblock copolymer, 2.3 wt% SEBS triblock copolymers, and 95.4 wt% light mineral oil. The polymer solution is heated to 110 °C under continuous mechanical stirring from a magnetic stir bar for ~1 h or until the polymers fully dissolve in the oil. The heat source is subsequently removed, and the polymer solution is cooled to ambient conditions under continuous stirring. Packed micelles solutions are prepared following similar protocols with polymer concentrations of 1.9 wt% SEP diblock copolymer, 1.9

wt% SEBS triblock copolymer, and 96.2 wt% light mineral oil. Prior to use, the samples are centrifuged for 30 s at 3000 RPM to remove any air bubbles present.

1.3. 3D Printing

All microbeams are 3D-printed using a custom-built 3D-printer consisting of a piezo-electric linear stage as a syringe pump (Physik Instrumente) attached to three linear translational stages (Newport) providing motion in the X, Y, and Z directions. The printed inks are loaded into a glass syringe (Hamilton Gastight) equipped with a blunt metal needle (McMaster Carr) acting as the printing nozzle. The gauge size of the printing nozzle is varied depending on the diameter of the beam being printed such that the diameters of the printed beams are within a factor of 2 of the diameters of the printing nozzle. All microbeams are printed at a linear translational speed of v_n = 10mm/s; the feature size of the printed object was controlled through changes in the volumetric flow rate of the material as set by the translational speed of the syringe pump. Both the syringe pump and the translational stages of the 3D-printer are controlled through custom-written Matlab scripts.

1.4. Rheological Characterization

Rheological characterization of the aqueous and organic materials is performed using an Anton Paar MCR 702 Rheometer equipped with a 25 mm roughened plate on plate configuration. Unidirectional shear rates sweeps are performed by ramping the shear rate from 500 s^{-1} – 10^{-3} s^{-1} and measuring the resulting shear stresses. Frequency sweeps are performed at 1% strain from 10^{1} – 10^{-2} Hz. The unidirectional shear rate sweeps are performed first to eliminate any residual stresses introduced during the loading of the sample.

1.5. Imaging

Macroscopic images and time-lapses of the printed structures are taken with a Nikon D3X camera and the DigiCam Capture image acquisition software. Data analysis is performed using ImageJ software and custom written Matlab scripts.

2. Supplemental Figures

2.1. Dominating timescale of elastic beam in viscous fluid

To determine the complex shear modulus of the viscous support bath as the aqueous microgel beams contract and deform we consider two timescales. The first timescale corresponds to the speed at which the elastic beam axially contracts. While the center of the beam can be considered stationary, either end of the beam will contract with a speed $v = \Delta L/2\Delta t$, where ΔL is the change in length of beam over the time interval Δt. We measure the total length of the microgel beam as it contracts from timelapse videos and calculate the maximum speed at which the beam contracts (Fig. S1). After an initial rapid contraction, the speed at which the beam contracts plateaus to a rate of < 5 μm/s. We note that both the undulating and buckling behavior of the beam is observed at these lower speeds. Furthermore, the speed measured here is the maximum speed of the beam; the contraction speed will decrease as you move toward the center of the beam in which the buckling behavior is observed.

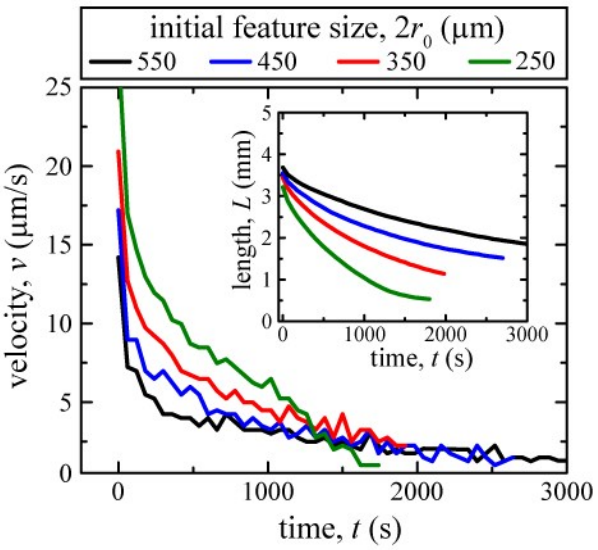

Figure S1. Contraction speed of the elastic beams within viscous fluids. The velocity of the contracting beam $v = \Delta L/2\Delta t$ is calculated by measuring the total length of the beam as a function of time (inset). After an initial rapid contraction, the speed at which the ends of the beam contract settle to rates $\sim<$ 5 μm/s.

The second timescale we consider corresponds to the speed at which the elastic beam sinks through the viscous fluid support material. We approximate this speed by balancing the buoyancy force driving the motion with the drag force resisting the motion of the sinking beam. The buoyancy force is given as $F_b = \Delta\rho Vg$, where $\Delta\rho$ is the density mismatch between the aqueous microgels and

the viscous support material, V is the volume of the printed beam, g is the gravitational constant. The resisting drag force is given as $F_d = \frac{1}{2}\rho v^2 A C_d$, where, v is the velocity in which the beam sinks, ρ is the density of the viscous support material, A is a geometrical constant, and C_d is the drag coefficient. For a cylinder, the geometric constant is given as $A = 2rL$. The drag coefficient is related to the Reynold's number and is given as $C_d = 24/\mathrm{Re}$, where $\mathrm{Re} = \rho v d/\eta$, and η is the viscosity of the viscous support bath. We solve the force balance for the velocity of the sinking beam and find the speed at which the beam sinks to be between 3 - 30 μm/s corresponding with a shear rate of ~ 0.07 s^{-1}. Thus, we conclude that the speed at which the elastic beam sinks through the viscous support material is the dominating timescale that sets the complex shear modulus of the viscous support material. We relate this measured shear rate to shear rates of our small amplitude frequency sweeps to determine the effective frequency, $\omega \approx 0.17$ Hz, and corresponding elastic shear modulus, $G' \approx$ 37 Pa, of the viscous support material.

2.2. Measuring Wavelength using Autocorrelation Analysis

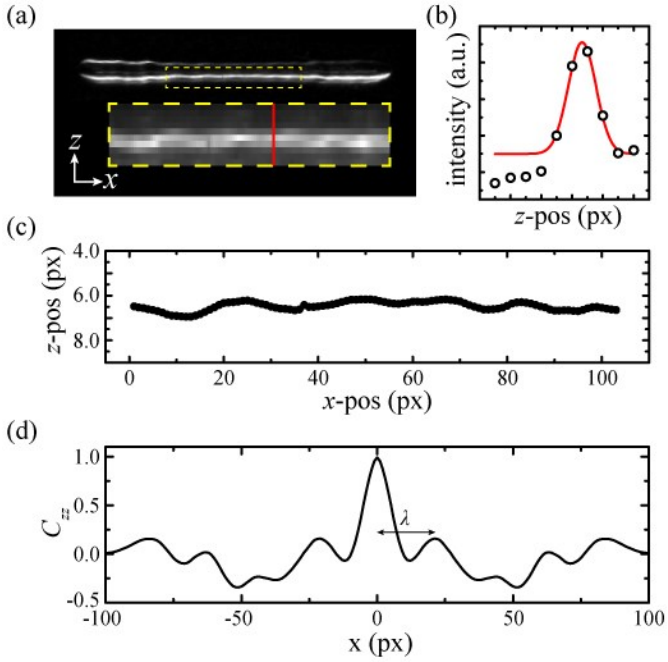

Figure S2. Measuring wavelength with autocorrelation analysis. The undulation and buckling wavelengths of the printed beams are measured using an autocorrelation analysis of the edge of the printed beam. **(a-c)** The region of interest is isolated from the macroscopic images and a gaussian curve is fit to the intensity at each x-position to determine the z-location of the beam edge. **(d)** The wavelength is determined by computing the autocorrelation of the edge position; the first peak location in the autocorrelation analysis corresponds with the wavelength of the printed beam.

2.3. Coiling wavelength

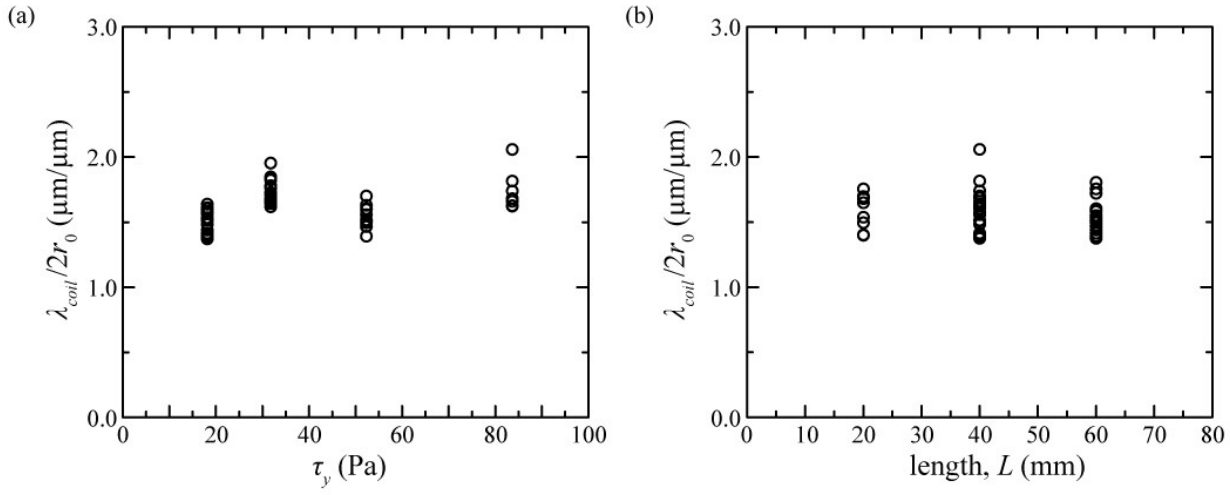

Figure S3. Wavelength measurements of printed beams undergoing coiling behavior. **(a)** The measured wavelength of the coiling beams decreases with increasing yield stress of the elastic beam. However, if we normalize the measure wavelength by the initial diameter of the printed beam, we find the measured wavelength is independent of the yield stress of the elastic beam. **(b)** Likewise, we find that the measured wavelength of the coiling beam normalized by the initial diameter of the beam is independent of the total length (L) of the printed beam.

2.4. Rayleigh-Plateau vs. Buckling Instability

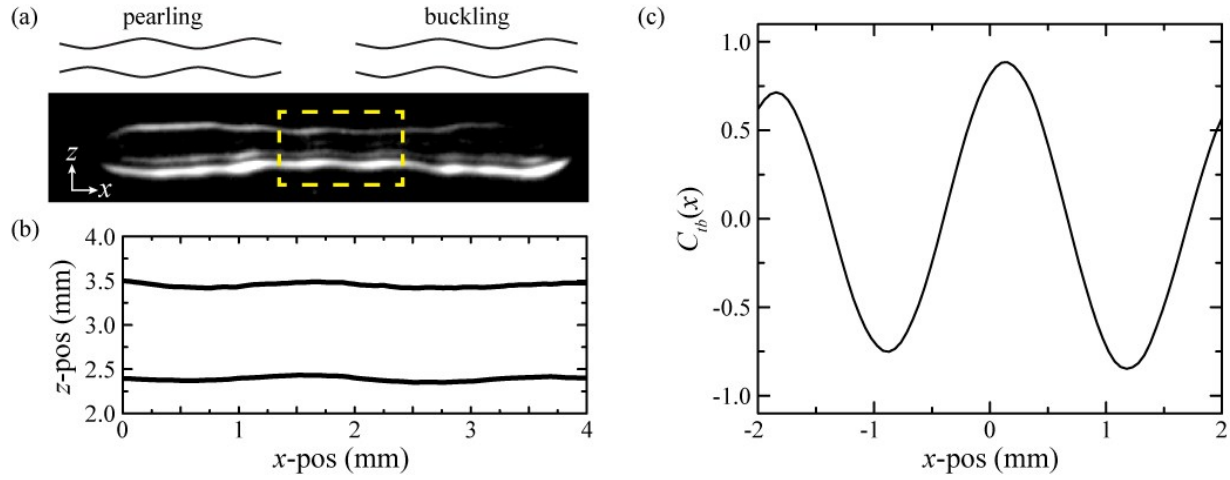

Figure S4. Undulation mechanism at the center of the beam. **(a)** To determine which mechanism may drive the observed undulation at the center of the beam, we compare the profiles of opposing surfaces of a deformed beam using cross-correlation analysis; a Rayleigh-Plateau instability will result in a pearling behavior in which the opposing undulations are out-of-phase with one another whereas the opposing surfaces of a buckling beam would exhibit undulations in-phase with one another. **(b)** The positions of the top and bottom edges are determined by fitting a gaussian curve to the intensity profile for each x-location. **(c)** Cross-correlation analysis between the top and bottom edge profiles show he undulation patterns to be in-phase with one another, suggesting that the undulation behavior results from a buckling instability.